

Labeling Ribonuclease S with a 3 nm Au Nanoparticle by Two-Step Assembly

Marie-Eve Aubin,[‡] Diana G. Morales,[‡] and Kimberly Hamad-Schifferli^{*,†,‡}

Department of Mechanical Engineering and Biological Engineering Division,
Massachusetts Institute of Technology, 77 Massachusetts Avenue,
Cambridge, Massachusetts 02139

Received December 17, 2004; Revised Manuscript Received February 2, 2005

ABSTRACT

We label ribonuclease S with a 3 nm Au nanoparticle (NP) by utilizing its two-piece structure. One portion, S-peptide, is mutated with a unique NP attachment site. NP-peptide self-assembles with the other portion, S-protein, to form an active enzyme. NP mobility decreases with peptide labeling and S-protein association. Surface plasmon shifts support conjugation. Higher S-peptide coverages on the NP surface reduce nonspecific adsorption, while sterically hindering assembly of RNaseS. Thiols displace nonspecific adsorption, maximizing site-specific labeling.

Au nanoparticle (NP) labeling of biomolecules is important for applications in imaging¹ sensing,^{2,3} assembly,⁴ and control.⁵ NP labeling of DNA has been facilitated by widely available and diverse chemical modification of DNA in such a way that does not interfere with its function, i.e., forming a hybrid pair. Consequently, labeling DNA of NPs is much more advanced in that the ratio between NP and DNA and oligo conformation can be quantified and controlled.^{6–8} Proteins are more difficult to functionalize with NPs as they have numerous chemical interactions and thus a greater possibility for nonspecific adsorption. Also, it is difficult to introduce a unique cysteine that can interact with the NP, as typically proteins possess multiple cysteines, primarily as disulfide bridges. Furthermore, proteins have a complex three-dimensional structure that must be preserved for function. For applications of NP–protein conjugates, it is crucial that labeling does not modify active site structure, so site-specific labeling is desirable. Therefore, conjugation of a protein with NP presents major challenges. Previously, NPs have been linked to enzymes such that activity is retained, but often electrostatic interactions have been utilized, so the site of attachment is difficult to control precisely. So far there have been only a few experiments that address the conformation of proteins linked to nanoparticle surfaces.^{3,9} In addition, it is found that certain proteins are particularly robust to nonspecific adsorption and upon conjugation to NPs, where the protein retains its general size and shape. However, one would like not to be restricted to NP conjugation of robust or nonenzymatically active proteins (such as structural proteins), particularly if the application

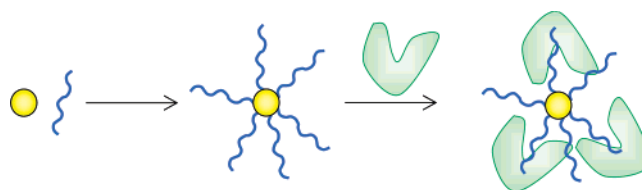


Figure 1. Strategy for labeling RNase S via a two-step reaction. Au NPs are first linked to the S-18 peptide (blue) that possesses a unique cysteine. The NP–S18 conjugate is then incubated with S-protein (green) to yield a fully formed complex.

of the NP–protein conjugate is for sensing or control. Therefore, a route for linking NPs to proteins at a unique site in such a way that nonspecific adsorption can be assessed and controlled needs to be explored.

We demonstrate here a method that simplifies protein conjugation to NPs by taking advantage of a protein that is made of two pieces, ribonuclease S (RNase S, Figure 1). The short piece is a 15–20 residue peptide, which can be easily appended with a unique labeling site and is thus much easier to conjugate to a NP and subsequently purify. The peptide self-assembles with the other portion of the protein to form a fully active enzyme. This strategy does not require cloning techniques to introduce unique sites, and methods used to optimize DNA–NP conjugation can also be applied.

RNase A is an extensively studied enzyme which has 124 residues (13.7 kD) and cleaves RNA pyrimidines by acid–base catalysis. RNase S is a form of RNase A in two pieces: a short piece of 20 residues, the S-peptide, plus the rest of the enzyme, the S-protein (104 residues). The S-protein and S-peptide spontaneously associate to form an active enzyme,¹⁰ and S-peptide or S-protein alone exhibits no enzymatic activity. The two portions have a dissociation

* Corresponding author. E-mail: schiffer@mit.edu.

[†] Department of Mechanical Engineering.

[‡] Biological Engineering Division.

Table 1. S-Peptide Sequences

name	sequence
S18	CGG KETAAAKFER QHMDS
S19	KETAWAIFVR QHMDSSTSA
wild-type S-peptide	KETAAAKFER QHMDSSTSA

constant of about 10^{-9} M, so S-peptides have been utilized as affinity tags for protein purification. Modification of S-peptide has been done extensively, both by mutagenesis and with chromophores and artificial groups for applications of control by light or chemical moieties.¹¹ Mutagenic studies have shown that S-peptide can be truncated to its 15 first residues or have residues added to the N-terminus without perturbing enzymatic function. Therefore, this permits extension of the S-peptide with a cysteine which provides a unique thiol on the S-peptide for linking to a Au NP. Two glycine spacers are also added (S18, sequence in Table 1, mutations in bold).

Water-soluble Au NPs were synthesized according to literature methods¹² and had a mean diameter of $3 \text{ nm} \pm 0.4 \text{ nm}$, determined by TEM. NPs were functionalized with the ligand bis(p-sulfonatophenyl) phenylphosphine dihydrate, dipotassium salt (BPS) in excess. S18 was synthesized commercially (Sigma-Genosys, purity 77%). The low yield on the synthesis was determined to be primarily due to dithiol linkages, evidenced by a dimer in the mass spectrometry data (not shown). NPs were linked to S18 by incubation in phosphate buffer ($1 \times$ PBS) for 1 h at 25°C . NP/S18 ratios in the reaction were 1:1, 1:5, and 1:25 with the NP concentration at $10 \mu\text{M}$. The NP-S18 conjugates were incubated with $1 \times$, $5 \times$, and $10 \times$ S-protein for 1 h at 25°C in phosphate buffer. Separation of NP/proteins was performed by agarose gel electrophoresis. Although sodium dodecyl sulfate (SDS) polyacrylamide gel electrophoresis (PAGE) is typically utilized for separations of proteins, it was not amenable for NP bioconjugates as SDS caused irreversible flocculation of the sample. Agarose gels were either 3 or 4 wt % in $0.5 \times$ TBE with field strength of 10 V/cm in $0.5 \times$ TBE running buffer.

If Au NPs are incubated with proteins that do not possess a surface thiol for linking, nonspecific adsorption is observed. Gel electrophoresis of $5 \mu\text{M}$ Au NPs incubated overnight with 1:10 RNase A, 1:10 cytochrome *c*, and 1:10 bovine serum albumin (Supporting Information) shows significant shifts of all bands toward lower mobility relative to Au-NP due to nonspecific adsorption with the NP, demonstrating the prevalence of this effect. In addition, S-protein incubated with NPs alone also shifts mobility (Figure 3a, lanes 5 and 9). These proteins have no exposed surface thiols but an abundance of lysines, which are known to stick to nanoparticle surfaces through the amine.^{3,13} It is possible that disulfide bridges can be broken to create SH groups that could link to the NP. Therefore, conjugation to systems that lack cysteines other than the site of labeling is desirable.

Figure 2 shows a gel where the NPs are linked to RNase S by the two-step method described in Figure 1. Lane 1 shows plain NPs. Lanes 2 and 3 are NP/S18 of 1:5, 1:25.

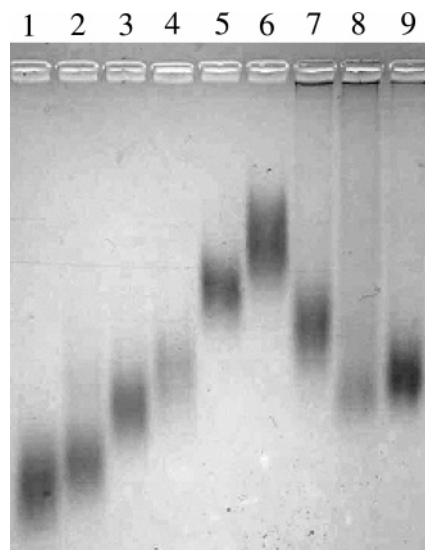


Figure 2. 4% agarose gel electrophoresis of 3 nm NP(1), incubated 1 h with S18 in a ratio of (NP/S18) 1:5 (2) and 1:25 (3), followed by 1 h incubation with S-protein in a NP/S18/S-protein ratio of 1:25:1 (4), 1:25:5 (5), and 1:25:10 (6). The 1:25:10 sample was subsequently incubated overnight with S19 in a concentration $50 \times$ [NP] (7). The S19 was incubated overnight with the 1:5 sample (8) and the 1:25 sample (9), in a concentration of $50 \times$ [NP].

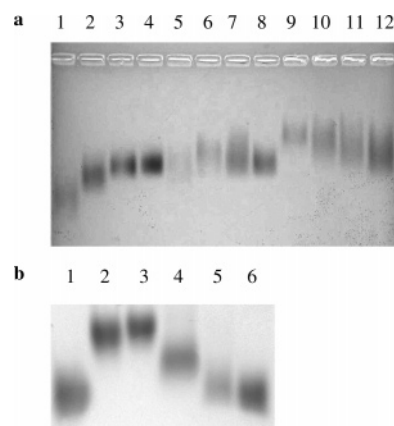


Figure 3. (a) Exploring the effect of NP/S18 ratio with 3% agarose gel electrophoresis. NP/S18/S-protein in ratios of 1:0:0 (lane 1), 1:5:0 (2), 1:25:0 (3), 1:50:0 (4), 1:0:1 (5), 1:5:1 (6), 1:25:1 (7), 1:50:1 (8), 1:0:10 (9), 1:5:10 (10), 1:25:10 (11), 1:50:10 (12). (b) MPA displacement of nonspecific adsorption on NP surfaces. 4% agarose gel of Au NPs (1), 1:25 NP:S18 (2), 1:25 NP:S18 with MPA (3), 1:25 NP:S19 (4), 1:25 NP:S19 with MPA (5), Au NPs with MPA (6).

Lanes 4–6 are 1:25 samples incubated with S-protein (NP/S18/S-protein ratios of 1:25:1, 1:25:5, 1:25:10). Addition of S-protein to the 1:25 shifts the mobility considerably, suggesting the S-protein is binding to the S18 and not the NP surface. Systematic increases of S18 followed by incubation with S-protein show that ratios of NP/S18 of approximately 1:25, both nonspecific adsorption and steric effects which hinder the attachment of S-protein, can be minimized (Figure 3a). Lanes 1–4 are increasing NP/S18 alone, lanes 5–8 are increasing NP/S18 with $1 \times$ S-protein, and lanes 8–14 are increasing NP/S18 with $10 \times$ S-protein. As the NP/S18 ratio is increased, incubation of S-protein

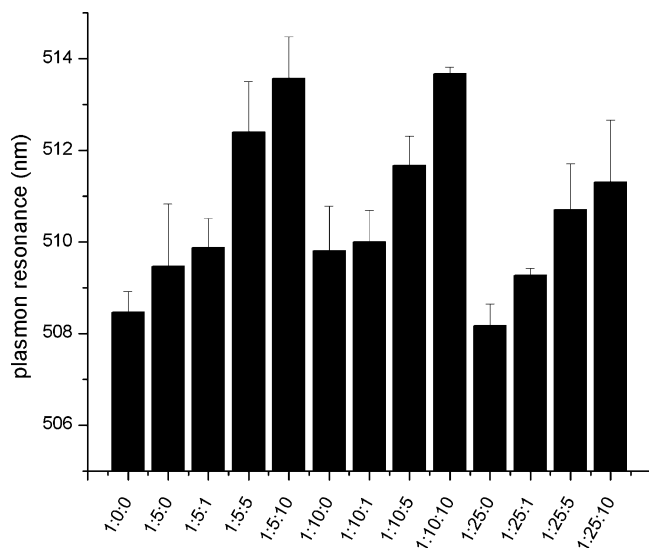


Figure 4. Surface plasmon resonance shifts for Au NPs with addition of S18 and S protein (NP/S18/S-protein). Peak maxima of the SPR feature as determined by optical absorption spectroscopy for different NP bioconjugates.

results in a smaller shift relative to the position of the NP–S18 without S-protein. This could be due to steric hindrance of S-protein binding to S18 on the NP surface at higher S18 coverages. It is known that the S-peptide has a random coil configuration but adopts an α -helical structure upon binding to S-protein.¹⁰ Presumably at these higher S18 coverages there is not enough space for the S18 to adopt the proper conformation, or for S-protein to get close enough to the S18 to properly bind.

In addition, a red shift of the Au NP surface plasmon resonance (SPR) is observed for the 1:5, 1:10, and 1:25 samples upon increasing amounts of S-protein added (Figure 4), an effect consistent with increasing amounts of protein on the NP surface.¹⁴ It should be noted that when comparing the 1:5, 1:10, and 1:25 SPR positions, higher amounts of S18 result in a blue shift. This may be due to a displacement of the BPS ligand by the thiol on S18. Comparable blue shifts are observed if the BPS ligands are displaced with the thiol mercaptopropionic acid ($\text{HS}(\text{CH}_2)_2\text{CO}_2\text{H}$, MPA) (data not shown).

To show that binding between the S-protein and S18 on the NP is specific, we performed a competition binding assay. S19 is a mutated S-peptide that binds $110\times$ more tightly to S-protein than the wild-type and which has no cysteines (sequence, Table 1).¹⁵ S19 was chemically synthesized (Sigma-Genosys) at a purity of 95%. S19 was incubated with the 1:25:10 sample overnight at $50\times$, and its gel mobility was compared to samples before exposure to S19. The 1:25:10:50 \times (NP/S18/S-protein/S19) band (Figure 2, lane 8) shifts forward relative to the 1:25 sample (lane 3), indicating that S19 has extracted S-protein from the S18 on the NP surface, with two to four S-proteins remaining on each NP.

Nonspecific interactions between proteins or DNA and Au surfaces or NPs are well known, and similar behavior with S18 is observed. Presumably, higher coverages would prevent nonspecific interactions, as less of the NP surface would be

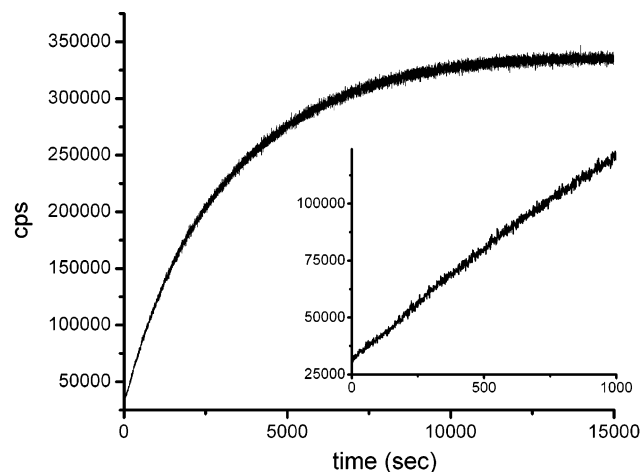


Figure 5. Enzymatic activity of NP/RNase-S for the 1:25:10 sample. Fluorescence intensity vs time for a 1:25:10 incubated with the substrate 5'-(6-FAM)-(dA)₃rU(dA)₄-(6-TAMRA)-3'. Inset: linear region at short times (0–1000 s).

exposed. Similar effects have been observed for DNA on NP surfaces.^{6,16} To explore how the NP/S18 ratio affects nonspecific adsorption, 1:5 and 1:25 samples were incubated overnight with $50\times$ S19. The 1:5 sample incubated with S19 (Figure 2, lane 8) is shifted to higher mobility relative to its original position in lane 2, indicating an interaction between the two species. However, the 1:25 incubated with S19 (lane 9) does not show an appreciable shift from its original position (lane 3). These observed mobility changes could be due to the 1:25 NP/S18 having a fully saturated surface, lacking room for S19 to nonspecifically adsorb.

Furthermore, strategies developed for DNA to displace nonspecific adsorption of the peptide can be utilized. Incubation with short-chain thiols has been used successfully for DNA on planar and NP Au surfaces.^{8,17} If 1:25 NP/S19 sample (Figure 3b, lane 4) are incubated with 1 mM MPA for 4 h (lane 5), the band shifts forward close to the plain NP position (lane 1), indicating displacement of the S19 nonspecifically bound to the NP. However, incubation of 1:25 NP/S18 (lane 2) with MPA under identical conditions (Lane 3) results in a negligible mobility change, suggesting that the covalently attached S18 to the NP does not get displaced. NPs incubated with MPA show no noticeable change in mobility (lane 6).

Activity of the NP-labeled RNase S was investigated. The bioconjugate was extracted from the gel in lanes 4 and 6 by spin centrifugation of gel slices and tested for activity by exposure to a substrate of a DNA oligo with a central RNA nucleotide, rU, the cleavage point for the enzyme (5'-(6-FAM)-(dA)₃rU(dA)₄-(6-TAMRA)-3', obtained from Pro-Logo). The FAM/TAMRA FRET pair on the ends enables fluorescence spectroscopy to probe strand cleavage. As the enzyme cleaves the strand at rU, FAM is no longer quenched by TAMRA, so FAM fluorescence increases.¹⁸ FAM emission of samples in $1\times$ PBS was measured by a fluorometer at room temperature. Fluorescence increases with time for Au–RNase S (1:25:10) at 50 nM with 15 nM substrate, demonstrating activity of the RNase S (Figure 5). Kinetic

analysis of the activity curves was performed using the equation

$$I = I_f - (I_f - I_0)e - (k_{\text{cat}}/K_M)[E]t \quad (1)$$

for long times and

$$I = I_0 + (I_f - I_0)(k_{\text{cat}}/K_M)[E]t \quad (2)$$

for the linear region at short times (inset, Figure 5).¹⁸ I_0 and I_f are the initial and final fluorescence intensities, respectively, and $[E]$ is the enzyme concentration. Conventionally, this yields a value for k_{cat}/K_M , the turnover rate per protein. However, protein concentration here cannot be accurately determined. Typically this is achieved by optical absorption, but the protein absorption at 280 nm is superimposed on top of the NP spectrum. This is further complicated by the fact that the protein molar extinction coefficient, ϵ , is at least 2 orders of magnitude lower than the NP, not accounting for the absorption of the NP ligand BPS. On the other hand, NP concentration can be determined using $\epsilon = 2.5 \times 10^6 \text{ M}^{-1} \text{ cm}^{-1}$ at the plasmon peak absorption, in the range of 508–515 nm, where the protein does not absorb. ϵ is obtained by calibration with known NP concentrations and correspondence with literature results. Therefore, we report a value for k_{cat}/K_M as the turnover rate per NP. The k_{cat}/K_M for the 1:25:1 sample is $1.39 \pm 0.04 \times 10^3 \text{ M}^{-1} \text{ s}^{-1}$ and $7.8 \pm 1.2 \times 10^3 \text{ M}^{-1} \text{ s}^{-1}$ for 1:25:10, a $5.5 \times$ increase. The k_{cat}/K_M of RNase S formed with S19 and S-protein under identical conditions was $5.8 \pm 0.8 \times 10^5 \text{ M}^{-1} \text{ s}^{-1}$, showing that labeling lowers enzyme efficiency by $100 \times$, possibly due to steric hindrance of the active site on the NP surface, which makes it difficult for the RNA substrate to properly bind and be cleaved.

Correspondence with the results from gel mobility allows estimation of the ratio of S-protein per NP. The k_{cat}/K_M of the 1:25:10 sample that has been incubated with $50 \times$ S19 is $2.5 \pm 0.6 \times 10^6 \text{ M}^{-1} \text{ s}^{-1}$. This is largely a measurement of the activity of the S19–S-protein complex, and its value implies that S19 can remove approximately 4–5 S-protein per NP. Based on the gel migration results in Figure 2, incubation of S19 with the 1:25:10 sample under identical conditions still leaves some S-protein bound to the NP–S18 complex. Assuming that the 1:25:5 sample has as an upper bound of 5 S-proteins per NP, and noting that the relative position of the 1:25:10 + $50 \times$ S19 lies between the 1:25:1 and 1:25:5 bands, it can be approximated that competitive binding with S19 leaves all but about 2–4 S-proteins per NP. Therefore, the 1:25 sample has the capacity to bind approximately 8 S-proteins/NP. Again, the observed increase in activity of only $5.5 \times$ between the 1:25:1 sample and the 1:25:10 instead of a $7\text{--}9 \times$ increase, which

could possibly be explained by steric hindrance on the NP surface. Further work investigating structure of the protein and quantifying the NP:RNase S stoichiometry is being pursued.

In summary, a strategy for labeling a protein made of two portions is described. Nonspecific adsorption arguments similar to those employed for DNA justify the first step of this approach, consisting of assembling a monolayer of mutated S-peptide (S18) on Au NP. As steric effects were found to hinder the correct assembly of RNaseS on NPs, an optimum S18 coverage is determined. The protein remains active after labeling with the NP. The measured lower turnover rate is most likely due to crowding between the S18 on the NP surface, which could impede the RNA in reaching the active site.

Acknowledgment. D.G.M. was supported by the NSF BPEC REU fellowship.

Supporting Information Available: (1) Gel electrophoresis of NP-protein conjugates; (2) Conjugation Au NPs to other proteins; (3) MPA treatment; (4) Gel electrophoresis; (5) Optical absorption spectroscopy; and (6) Fluorescence spectroscopy. This material is available free of charge via the Internet at <http://pubs.acs.org>.

References

- (1) Hainfield, J. F.; Powell, R. D. *J. Histochem. Cytochem.* **2000**, *48*, 471–480.
- (2) Taton, A. T.; Mirkin, C. A.; Letsinger, R. L. *Science* **2000**, *289*, 1757–1760.
- (3) Keating, C. D.; Kovaleski, K. M.; Natan, M. J. *J. Phys. Chem. B* **1998**, *102*, 9404–9413.
- (4) Niemeyer, C. M. *Angew. Chem., Int. Ed. Engl.* **2001**, *40*, 4128–4158.
- (5) Hamad-Schifferli, K.; Schwartz, J. J.; Santos, A.; Zhang, S.; Jacobson, J. M. *Nature* **2002**, *415*, 152–155.
- (6) Parak, W. J.; Pellegrino, T.; Micheel, C. M.; Gerion, D.; Williams, S. C.; Alivisatos, A. P. *Nano Lett.* **2003**, *3*, 33–36.
- (7) Zanchet, D.; Micheel, C. M.; Parak, W. J.; Gerion, D.; Alivisatos, A. P. *Nano Lett.* **2001**, *1*, 32–35.
- (8) Park, S.; Brown, K. A.; Hamad-Schifferli, K. *Nano Lett.* **2004**, *4*, 1925–1929.
- (9) Medintz, I. L.; Konnert, J. H.; Clapp, A. R.; Stanish, I.; Twigg, M. E.; Matoussi, H.; Mauro, J. M.; Deschamps, J. R. *Proc. Natl. Acad. Sci. U.S.A.* **2004**, *101*, 9612–9617.
- (10) Labhardt, A. M. *Proc. Natl. Acad. Sci. U.S.A.* **1984**, *81*, 7674–7678.
- (11) Liu, D.; Karanicolas, J.; Yu, C.; Zhang, Z. H.; Woolley, G. A. *Bioorg. Med. Chem. Lett.* **1997**, *7*, 2677–2680.
- (12) Jana, N. R.; Peng, X. *J. Am. Chem. Soc.* **2003**, *125*, 14280–14281.
- (13) Leff, D. V.; Brandt, L.; Heath, J. R. *Langmuir* **1996**, *12*, 4723–4730.
- (14) Gole, A.; Dash, C.; Soman, C.; Sainkar, S. R.; Rao, M.; Sastry, M. *Bioconjugate Chem.* **2001**, *12*, 684–690.
- (15) Dwyer, J. J.; Dwyer, M. A.; Kossiakoff, A. A. *Biochem.* **2001**, *40*, 13491–13500.
- (16) Storhoff, J. J.; Elghanian, R.; Mirkin, C. A.; Letsinger, R. L. *Langmuir* **2002**, *18*, 6666–6670.
- (17) Mbindyo, J. K. N.; Reiss, B. D.; Martin, B. R.; Keating, C. D.; Natan, M. J.; Mallouk, T. E. *Adv. Mater.* **2001**, *13*, 249–254.
- (18) Kelemen, B. R.; Klink, T. A.; Behlke, M. A.; Eubanks, S. R.; Leland, P. A.; Raines, R. T. *Nucleic Acids Res.* **1999**, *27*, 3696–3701.

NL0479031